Preparation of biomimetic photoresponsive polymer springs

Supitchaya Iamsaard[1], Elise Villemin[2], Federico Lancia[1], Sarah-Jane Aβhoff[1], Stephen P Fletcher[2] & Nathalie Katsonis[1]

[1]Bio-inspired and Smart Materials, MESA+ Institute for Nanotechnology, University of Twente, Enschede, the Netherlands. [2]Department of Chemistry, Chemistry Research Laboratory, University of Oxford, Oxford, UK. Correspondence should be addressed to S.P.F. (stephen.fletcher@chem.ox.ac.uk) or N.K. (n.h.katsonis@utwente.nl).

Published online 1 September 2016; doi:10.1038/nprot.2016.087

Polymer springs that twist under irradiation with light, in a manner that mimics how plant tendrils twist and turn under the effect of differential expansion in different sections of the plant, show potential for soft robotics and the development of artificial muscles. The soft springs prepared using this protocol are typically 1 mm wide, 50 μm thick and up to 10 cm long. They are made from liquid crystal polymer networks in which an azobenzene derivative is introduced covalently as a molecular photo-switch. The polymer network is prepared by irradiation of a twist cell filled with a mixture of shape-persistent liquid crystals, liquid crystals having reactive end groups, molecular photo-switches, some chiral dopant and a small amount of photoinitiator. After postcuring, the soft polymer film is removed and cut into springs, the geometry of which is determined by the angle of cut. The material composing the springs is characterized by optical microscopy, scanning electron microscopy and tensile strength measurements. The springs operate at ambient temperature, by mimicking the orthogonal contraction mechanism that is at the origin of plant coiling. They shape-shift under irradiation with UV light and can be pre-programmed to either wind or unwind, as encoded in their geometry. Once illumination is stopped, the springs return to their initial shape. Irradiation with visible light accelerates the shape reversion.

INTRODUCTION

Incorporation of molecular photo-switches in soft matter promises a route to smart materials that change their shape under illumination with light[1–3]. Engineering of large, complex and versatile shape transformations would allow the delivery of future materials that can produce work and, eventually, powerful movement, with potential applications in soft robotics and artificial muscles. The design, production and operation of functional smart photo-actuators thus constitute a major thrust of contemporary materials research, and biological materials have provided inspiration for relevant engineering paradigms. In nature, twisting and turning behaviors are widely used macroscale deformation modes that allow plants to achieve complex mechanical functions (**Fig. 1**). Cucumber tendrils coil and wind via asymmetric contraction of an internal fiber ribbon of specialized cells[4], seed pods open via a mechanism creating helical chirality[5], stems twine by producing a helical tweezing force[6] and seeds burrow into soil, as their helical bristles wind and unwind with daily cycles that change with ambient humidity[7]. Understanding and learning how to engineer systems displaying these types of highly controlled helical shape transformations would provide the capacity and incentive to design active materials with specific helix-based functionality.

Various strategies have been developed to mimic the shape shifting of biological springs, primarily by transforming bi-dimensional polymer-based films into 3D helix-based structures (**Supplementary Table 1**). Approaches based on polymer hydrogels provide springs that are pre-programmed to respond to changes in temperature or swell in response to an increase in humidity. Studart and colleagues[8] have developed a strategy based on the temperature-dependent hydration of gelatin, alginate or other polymers that were reinforced with inorganic platelets having varying orientations within the material. The orientation of these reinforcing elements determines the directionality of swelling and thus promotes a winding motion. The strong reversible hygroscopicity of agarose-based hydrogels has been combined with anisotropic networks of glass fibers, and it has shown potential for fast spiraling and twisting motion driven by changes in humidity, at room temperature[9,10]. Other hydrogel springs that respond with deformation to changes in temperature were developed by implementing alternating bar-like regions of different hydrogels with differential swelling[11]. In humidity-responsive materials, asymmetry in swelling can also be programmed by introducing salts selectively, on one side of the film only[12]. Actuation mechanisms based on swelling make sense in terms of biomimetic character, because many plants move in response to the daily cycle of humidity. However, the use of humidity as a trigger remains a limitation in terms of applications, and deswelling procedures can compromise the structural integrity of the material.

Light as a stimulus is compatible with a wide range of condensed phases; the kinetics of the photoresponse can usually be controlled by light intensity, and moreover light allows both spatial and temporal control over soft matter[3]. Here we report a bioinspired design strategy based on the use of liquid crystal polymer networks that are doped with molecular photo-switches. Specifically, we encode orthogonal deformation modes in thin films of liquid crystal polymer networks, and combine this asymmetric deformation with a differential stiffness that runs through the thickness of the film, in order to form spring-like materials that respond to irradiation with light. We optimize the mechanical properties of the springs by adjusting the composition of the pre-polymer liquid crystalline mixture (**Fig. 2**). The shape and photoresponse of the springs depend on a number of factors, including not only the composition of the polymer network but also the preparation procedure and the thickness of the film. This high sensitivity to variations in procedure can constitute a limitation that the present protocol is meant to address.

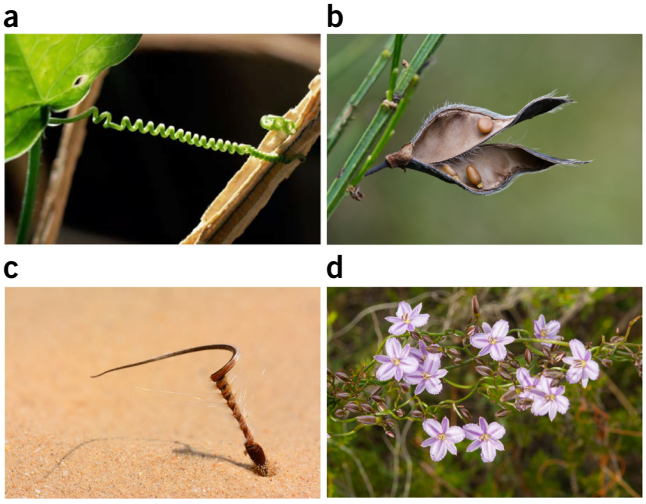

Figure 1 | Helix-based motion and mirror-image helices in biological systems. (**a**) Passion flower tendril. The twisting appears to originate in the asymmetric contraction of cellulose microfibrils. Science Photo Library/Alamy Stock Photo. (**b**) Common broom (*Sarothamnus scoparius*) seedpods. Seedpods open via a mechanism creating helical chirality. Krystyna Szulecka/Alamy Stock Photo. (**c**) Seed and awn of *Erodium*. The awns display humidity-driven helical motion. Itsik Marom/Alamy Stock Photo. (**d**) Twining fringe lily. Robert Wyatt/Alamy Stock Photo.

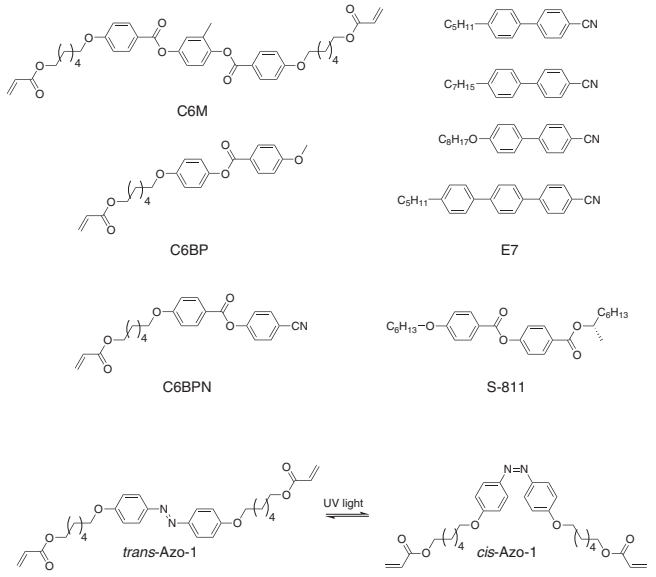

Figure 2 | Molecular omponents of the materials used in the experimental design.

We demonstrate that UV light induces structural changes at the molecular level, and we also show how these molecular transformations are converted into large-amplitude shape shifting. Once illumination with UV light is stopped, the springs return to their initial shape in ambient light conditions. Irradiation with visible light accelerates the shape reversion. This approach provides a versatile protocol, as a large number of shapes can be formed in one single sheet of materials.

Development of the protocol

We have started a research program that aims to mimic the mechanical movements seen in living systems using artificial responsive materials. At the heart of this research is the idea that the helical designs seen in nature are ideal for translating and amplifying deformation modes in artificial systems as well. We recently reported synthetic systems capable of translating molecular movement across scale lengths into macroscopic rotational movements that could serve as the basis of light-driven functional materials[13]. We have demonstrated that a variety of complex deformations are possible, including winding, unwinding and helix inversion, and that devices can be constructed to move macroscopic objects. Our bioinspired springs are based on liquid crystal polymer networks that incorporate azobenzene photo-switches covalently. When azobenzene photo-switches are in their stable *trans* form, their rod-like shape does not disrupt the liquid crystalline order, the molecules that form the liquid crystal orient in one direction preferentially and the polymer chains are elongated. When they are subjected to light, photoisomerization of the switches into their bent *cis* form disrupts the liquid crystalline order, and the polymer chains recover a random coiled conformation in an entropically favored process. The individual changes in the shape of the polymer chains translate to the macroscopic level, and overall this mechanism induces an anisotropic deformation of the material: light-induced shrinkage occurs primarily along the direction of preferential alignment of the liquid crystal molecules (called the director)[14].

We have shown that the mechanical properties of light-responsive liquid crystal polymer springs can be engineered by adjusting the following parameters:

(i) *Their aptitude to deform without breaking.* This relates to their cross-linking density, which itself relates to the ratios between acrylate and diacrylate liquid crystals forming the network[15] and to the proportion of nonpolymerizable molecules in the mixture.

(ii) *A gradient of stiffness through the thickness of the film.* Such a gradient is introduced during photopolymerization. This results in the two surfaces of the film having different mechanical properties—the less deformable surface will be found on the outside of the helically shaped ribbon preferentially, once the polymer spring is formed.

(iii) *The proportion of switches in the liquid crystal polymer network.* This proportion must be sufficiently low for light to penetrate the thin film, but the concentration of switches should be sufficient to efficiently disrupt the order of the polymeric material.

(iv) *The cutting direction.* This fixes the molecular orientation within the ribbon. Thus, in combination with the material's chirality and stiffness across the sample's thickness, the cutting direction determines the geometry and the photoactuation properties of the springs (**Fig. 3**).

Experimental design

Our design is based on the use of liquid crystal polymer networks that are characterized by their anisotropy; this feature is relevant because, in nature, plants use anisotropic expansion as a mechanism of movement. Specifically, plants expand perpendicularly to the orientation of fibrils when tissue swells in response

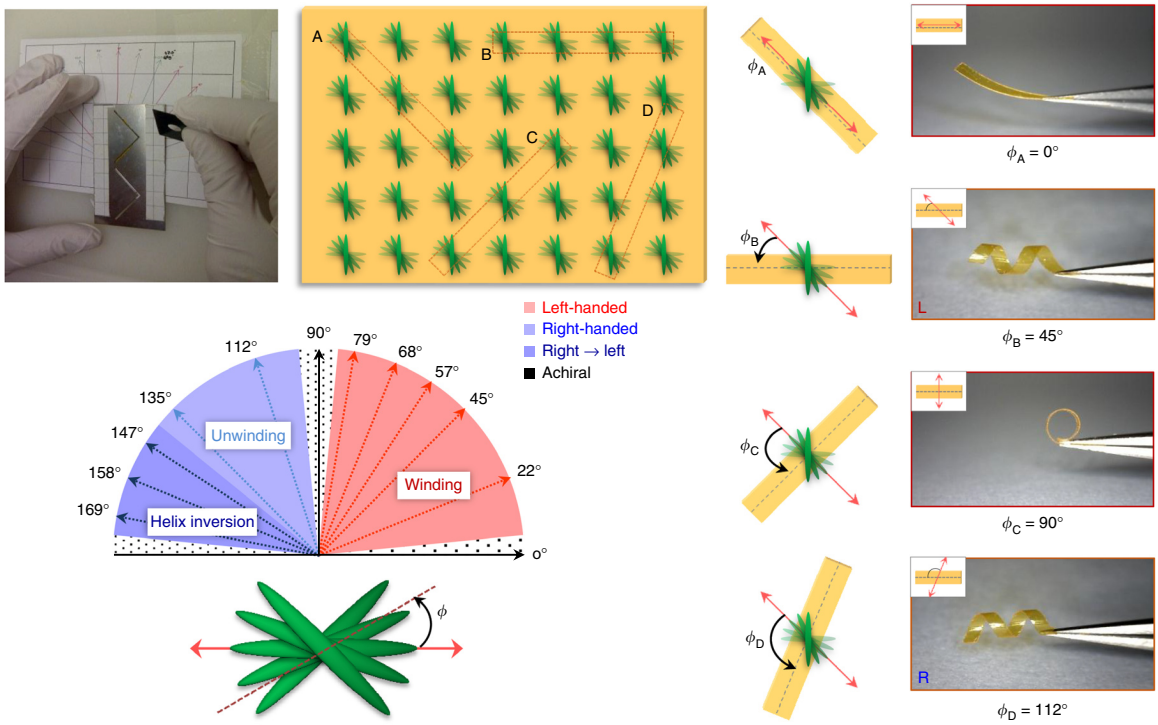

Figure 3 | A variety of springs can be prepared by cutting thin stripes in a homogeneous thin film of liquid crystal polymer network (top panel). The shape of the springs is reported as a function of the cutting angle ϕ (bottom and right panels).

to higher humidity[16]. Helix-based movement in plants, whether explosive release of strain or slow coiling motion, is a complex mechanism; the specifics are still under debate, but the deformation mechanism is usually based on a common principle: the orientation of cellulose microfibrils varies across the thickness of the plant, so when the tissue swells it expands in different directions, creating a curvature[17–19]. In pinecones and in the seedpods of orchid trees, cellulose microfibrils are oriented perpendicularly at each side of the plant tissue[8]. The asymmetric contraction induced by differential orientation can be further influenced by differential lignification of the cells, which introduces gradients in stiffness, with the stiffer region showing propensity to locate at the outer side of the curvature[20].

A twist cell to encode orthogonal deformation modes. We take advantage of the high sensitivity of liquid crystals to boundary conditions in order to reproduce differential deformation modes artificially. We use a cell composed of two glass slides, each of them covered with a thin polymer film that promotes the alignment of the liquid crystal in a specific direction: at the top of the cell the rod-like molecules are preferentially oriented along the short axis of the cell, whereas at the bottom of the cell the molecules are preferentially oriented along its long axis. These boundary conditions promote the formation of a 90° twist through the thickness of the cell, and the cell is referred to as a twist cell. The use of a twist cell to create a twist across the thickness of the cell is key in preparing spring-like actuators (**Fig. 4**)[21–23]. A small amount of chiral dopant is used to make sure that the twist has the same handedness over the whole sample and thus to secure cooperative effects in the film. In principle, any chiral dopant can be used, provided that it is miscible with the liquid crystal; it is preferable that it have a moderate helical twisting power (other groups have reported the use of dopants such as S-811 (ref. 21) or R-1011 (ref. 24)). At low concentrations, the chiral dopant promotes a twist that is proportional to its concentration. By choosing the right concentration, the twist is adjusted to match four times the thickness of the cell.

Origin of asymmetry. Three sources of asymmetry contribute to shape generation and actuation in this experimental design: (i) the angular offset that is introduced by cutting the ribbon at a specific angle ϕ, (ii) the handedness of the twist in the cell and (iii) a gradient in cross-linking density of the liquid crystal network that runs across the thickness of the film. The gradient is formed during cross-polymerization, by irradiating the liquid crystal in the twist cell, from one side of the cell exclusively[25]. After cross-polymerization, the cell is opened. The thickness of the ribbons corresponds well to the nominal thickness of the cell, as estimated by using scanning electron microscopy images of their cross-sections (**Supplementary Fig. 1**). Shrinkage of ~15% in the thickness of the film was observed upon cross-linking. Once ribbons are cut out of the liquid crystal polymer film, they spontaneously curl into springs as a result of the orthogonal shrinking that occurs during cross-polymerization[26]. In fact, we can produce a variety of chiral and achiral shapes, depending on the offset angle ϕ, which is defined as the angle between the average orientation of the molecules at midplane and the cutting direction (**Fig. 3**).

Composition of the liquid crystal polymer network. The composition of the liquid crystal must be adjusted to tune the properties of the springs in terms of their stiffness, shape and response to UV light (**Table 1**). The photo-switch Azo-1 is incorporated into the liquid crystal polymer network in its *trans* form, via two reactive end groups. The monomers that are used in polymerization

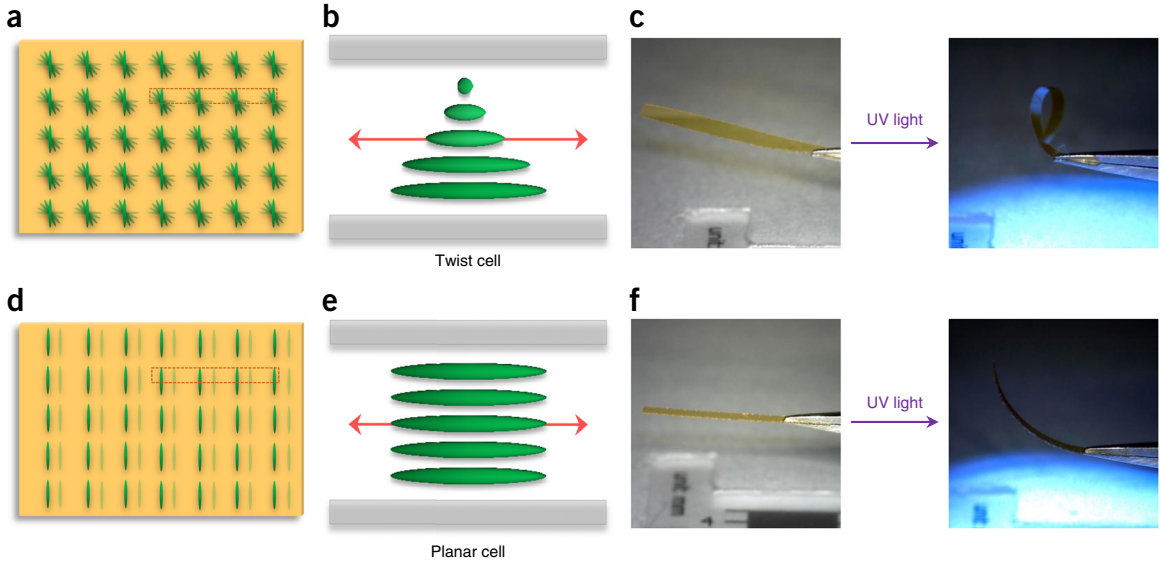

Figure 4 | A specific liquid crystal cell is required to prepare liquid crystal polymer springs. (**a**) A twist cell is filled with a liquid crystal of composition 4, **Table 1.** The green rods represent the liquid crystal molecules schematically and the distribution of their preferential orientation through the thickness of the film. The red rectangle shows the cutting edges for the ribbon shown in **c**. (**b**) A side representation of a twist cell. (**c**) The ribbon cut at $\phi = 45°$ twists under irradiation with light. (**d**) A planar cell filled with a liquid crystal of composition 4, **Table 1.** The red rectangle shows the cutting edges for the ribbon shown in **f**. (**e**) A side representation of a planar cell. The liquid crystal molecules are preferentially oriented in the same direction. (**f**) When a planar cell is used with the same offset angle ($\phi = 45°$), a flat ribbon bends under irradiation with light, but it does not twist.

have either one reactive end group (C6BP and C6BPN) or they act as cross-linkers with two reactive end groups (C6M; **Fig. 2**). It has been observed that incorporating a high ratio of cross-linking units into the network reduces the *trans*-to-*cis* photo-conversion and thus the amplitude of photoinduced deformation[15]. Moreover, a high ratio of cross-linkers promotes the formation of densely cross-linked polymer networks that are less deformable and less prone to forming springs. Therefore, we kept the proportion of cross-linker in the network as low as possible, typically lower than in previous works, and we introduced a relatively long spacer in the structure of C6M (**Fig. 2**). Some compositions provided fragile and breakable liquid crystal polymer films. We used E7, a well-known nematic liquid crystal that is a mixture of cyano-biphenyl derivatives (**Fig. 2**), in order to promote the formation of a loosely cross-linked and thus flexible polymer network. Eventually, the optimal composition that we designed is mixture 3 (ref. 13). Preparation of cross-linkable liquid crystal 3 is described in the procedure section. Differential scanning calorimetry of mixture 3 (without photoinitiator) shows a classic liquid crystalline behavior, with a nematic to isotropic transition occurring at 64.8 °C (**Supplementary Fig. 2**).

In the absence of Azo-1, springs were formed, but no photoresponse was ever observed at room temperature. The springs obtained from mixture 2 are stiff, and they also show no photoactuation. Adding E7 and adjusting the ratio between these nonpolymerizable molecules and the reactive monomers results in a marked improvement in the quality of the curled and twisted shapes obtained intitially, and in their photoresponsive properties as well (mixture 3). Lowering the concentration of photo-switches decreases the photoreactivity of the springs. Increasing the concentration of Azo-1 to values >10 wt% does not improve the photoresponse of the material because of the large absorption of light by the polymeric network.

The cutting angle determines the shape and photo-mechanical properties. Depending on the angle at which the ribbons are cut, different shapes are formed, including chiral shapes such as left-handed or right-handed springs, and, for some cutting directions, nonchiral ribbons (flat ribbons or open rings) are also formed. When the chiral dopant S-811 is replaced by its enantiomer R-811, the shape of the ribbons is a mirror image. For example, the left-handed helix cut for S-811 with $\phi = 33°$

TABLE 1 | Shape and photoresponse of liquid crystal polymer springs with different compositions.

Composition no.	C6M (wt%)	C6BP (wt%)	C6BPN (wt%)	E7 (wt%)	S-811 (wt%)	Azo-1 (wt%)	Shape	UV actuation
1	19.07	28.60	9.54	41.75	0.04	—	Curled	None
2	32.49	48.73	16.24	—	0.04	2.00	Flat	None
3	21.18	31.78	10.59	25.41	0.04	10.00	Curled	Yes
4	22.37	33.56	11.19	26.84	0.04	5.00	Flat	Low

Each of these compositions also incorporates up to 1 wt% of the photoinitiator Irgacure 819.

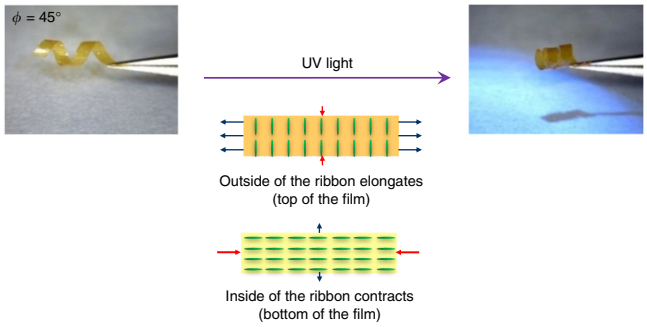

Figure 5 | Photo-actuated twisting and/or untwisting motion is encoded via orthogonal deformation modes: in all cases, the outside of the ribbon deforms perpendicularly to the inside of the ribbon. Specifically, in the example of a ribbon cut at $\phi = 45°$, the outside of the ribbon elongates, whereas its inside layer primarily contracts, which overall leads to twisting along its long axis upon irradiation with light at $\lambda = 365$ nm. The green rods schematically represent the preferential alignment of the liquid crystal molecules. The composition of this specific ribbon is described as composition 3 in **Table 1**.

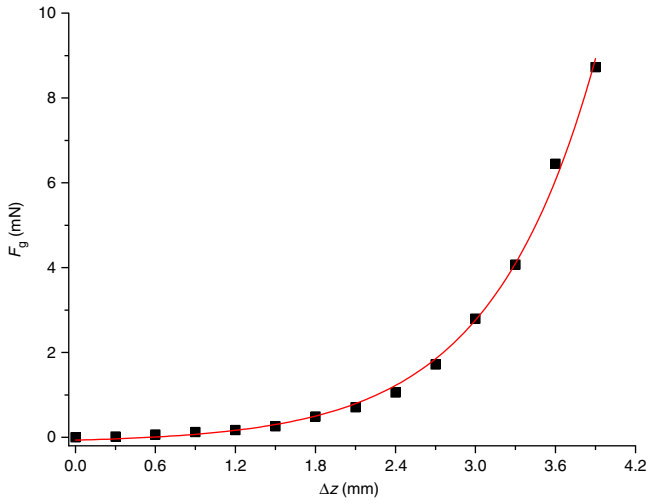

Figure 6 | Nonlinear mechanical character of a biomimetic photoresponsive polymer spring ($\phi = 45°$). The graph displays the pulling force that is applied to the spring with respect to its elongation. F_g, force applied by gravity to the spring.

is the enantiomer of an R-811 ribbon cut at $\phi = 147°$ (right-handed helix with the same pitch as the aforementioned helix)[13]. Upon irradiation with UV light, three different actuation modes are observed: winding ($\phi = 45°$, **Supplementary Video 1**), unwinding ($\phi = 112°$, **Supplementary Video 2**) and helix inversion ($\phi = 158°$, **Supplementary Video 3**). The actuation modes are encoded by design in the initial shape of each ribbon. For example, a ribbon cut at $\phi = 45°$ will undergo elongation of its outside surface and shrinkage of its inside surface, leading to an overall twisting motion upon appropriate irradiation with light (**Fig. 5**).

Design of the molecular switch. The best-performing photo-switches will be those that absorb light efficiently, are fast and undergo large geometrical changes that will efficiently generate disorder in the liquid crystal network[27]. Currently, azobenzene photo-switches are used primarily to actuate liquid crystal polymer networks, because in their bent *cis* form they disrupt the liquid crystalline order effectively. Different variations in the connectivity of the photo-switches have been explored, and studies have suggested that switches used as cross-linkers are more efficient than switches that are incorporated as dangling bonds. The length of the spacers separating the rigid core of the liquid crystal molecules from the reactive end-groups is known to influence the coupling between the photoisomerization of the switches and eventually the macroscopic deformation of the liquid crystal polymer network[28]: the mechanical response of the system is enhanced if the spacers are longer, up to a threshold length value. Further, the activation wavelength of the springs can be adjusted by molecular engineering of the azobenzene photo-switches[29,30].

Mechanical properties of the biomimetic springs. The stiffness of the springs was measured with a custom-made setup in which the spring is clamped on one side and pulled on the other side to force its elongation (**Supplementary Fig. 3**). Here we report the mechanical properties of a spring cut at $\phi = 45°$. Drawing the pulling force with respect to elongation of the spring yields the curve shown in **Figure 6**. For a specific elongation, the value of the stiffness corresponds to the tangent to this curve. Interestingly, our results show that the stiffness of the spring increases with the force that is applied to it—i.e., it behaves as a nonlinear spring, as observed in vertebrate muscle fibers[31]. The use of nonlinear springs is particularly attractive for robotic applications in human environments in which complex stiffness adjustment allows for a variety of tasks that are hardly feasible for conventional linear springs. Flat ribbons are capable of holding up to 3,000 times their weight and bearing a stress of up to 0.9 MPa.

Shape recovery of the biomimetic springs. When illumination with UV light is stopped, the springs relax back to their original shape ($\phi = 0°$, **Supplementary Video 4**). The kinetics of the shape recovery is determined by a balance between the elastic properties of the polymer network, the rate of relaxation of the *cis*-azobenzene and the coupling of the photo-switch to its environment. Typically, the half-life for relaxation of Azo-1 is ~15 min in ambient illumination conditions and a few hours in the dark. This relatively slow process can be accelerated by irradiation with intense visible light. Up to ten cycles of alternate UV and visible irradiation can be performed without evidence of degradation of the photo-mechanical properties.

MATERIALS

REAGENTS

- C6BP monomer: 4-methoxybenzoic acid 4-(6-acyloyloxy-hexyloxy)phenyl ester, 97% (Synthon Chemicals, cat. no. ST03866; **Fig. 2**)
- C6BPN monomer: 4[4[6-acyloxyhex-1-yl)oxyphenyl]carboxy-benzonitril, 97% (Synthon Chemicals, cat. no. ST02760; **Fig. 2**)
- C6M monomer: 1,4-bis[4-(6-acyloyloxyhexyloxylbenzoyloxy], 97% (Synthon Chemicals, cat. no. ST00975; **Fig. 2**)
- E7 liquid crystal (used as received; Merck Millipore, cat. no. T153-8927; **Fig. 2**)
- S-811 chiral dopant: *S*-octan-2-yl 4-((4-(hexyloxy)benzoyl)oxy)benzoate (Merck Millipore, cat. no. 111649; **Fig. 2**)

- Azo-1: photoresponsive Azo-1 was synthesized by following reported procedures for the formation of an azobenzene[32] and its connection to acrylate linkers[33] (**Fig. 2**)
- Photoinitiator: phenylbis(2,4,6-trimethylbenzoyl)phosphine oxide, 97.0% (Irgacure 819; Sigma-Aldrich, cat. no. 511447) **! CAUTION** The reagent is sensitive to visible light, and exposure to any light source should be avoided.
- Dichloromethane, HPLC grade (DCM; Sigma-Aldrich, cat. no. 270997)
- Nitrogen gas
- Liquid nitrogen **! CAUTION** Liquid nitrogen should be handled with cryogenic gloves in a well-ventilated environment.

EQUIPMENT

- Balances
- Utensils
- Hot plate (Präzitherm, Harry Gestigkeit)
- Magnetic stirring rod (7 × 2 mm)
- Metallic tip (lancet dissecting needle)
- Edmund MI-150 high-intensity illuminator (≈145 mW·cm^{-2})
- Cutoff filter ($\lambda \geq 420$ nm) Edmund Optics, 425 nm OD two long-pass filters, 50-mm diameter
- Oven
- Dewar flask
- Hönle Bluepoint light-emitting diode ($\lambda = 365$ nm, 38.62 mW·cm^{-2}, corresponding to 10% of the maximal intensity was used for all experiments)
- Dino-Lite Pro AM4113T USB camera (×29 magnification)
- Glass slides
- Polarized optical microscope (Olympus BX-51P, coupled to a digital camera (Olympus DP73))

Consumables

- Twist cell with a nominal 50-µm gap, ITO-covered, 10 × 5 mm, 90° (E.H.C., cat. no. KSRS-50/D607P1NSS)
- Planar cell with a nominal 50-µm gap, ITO-covered, 10 × 5 mm, 180° (E.H.C., cat. no. KSRP50/B107P1NSS)
- Brown glass vials
- Pasteur pipettes
- Aluminum paper

EQUIPMENT SETUP

Twist cell The cell walls should be covered with an LX-1400 (Hitachi-Kasei) polyimide layer (thickness within 20 nm). This alignment layer should be oriented by rubbing with the following specifications: a polyester fiber of 8 mm length, with a 58-mm roll diameter, 600 r.p.m. rotational speed, 30 mm/s stage speed and three times round-trip frequency.

Planar cell The cell walls should be treated as those of the twist cell.

PROCEDURE

Preparation of liquid crystal polymer thin films ● TIMING 1 d

1| Eliminate possible dust in vials and Pasteur pipettes by flushing with a nitrogen stream before use, as dust may generate defects in the liquid crystal films.

2| Weigh the solid components that are not sensitive to irradiation with light, 25.42 mg of C6M (21.18 wt%), 38.13 mg of C6BP (31.78 wt%) and 12.71 mg of C6BPN (10.59 wt%), in three separate vials and weigh 0.05 mg of chiral dopant S-811 (0.04 wt%) in another brown glass vial.

▲ **CRITICAL STEP** To avoid composition errors involving quantities of the chiral dopant S-811 in the transferring process, the vial containing S-811 should be used as a mixing vial, and all the other components should be transferred to this vial.

3| Weigh 30.50 mg of liquid crystal E7 using a pipette, in a separate vial.

4| Weigh the photosensitive component, 12.00 mg of photo-switchable monomer Azo-1 (10.00 wt%), in a separate brown glass vial to prevent photo-degradation.

5| Dissolve each component in a minimum volume of DCM, and, using pipettes, transfer them to the vial containing S-811. Rinse each vial three times with DCM. (The final volume should be ≈3 ml.)

6| Evaporate the DCM by using a stream of low-pressure nitrogen for 1 h. During this step, the vial should be on a hot plate heated at 60 °C, and the mixture should be protected from ambient light with aluminum foil. After all of the DCM has evaporated, the components that remain in the flask compose a liquid crystal.

▲ **CRITICAL STEP** Using a strong nitrogen stream tends to yield nonhomogeneous liquid crystalline mixtures (possibly associated with the crystallization of some monomers).

7| Weigh 1.20 mg of photoinitiator (Irgacure 819, 1.00 wt%) in a separate brown glass vial.

▲ **CRITICAL STEP** Manipulations involving the photoinitiator have to be performed in the dark.

8| Dissolve the photoinitiator in a minimum volume of DCM and add it to the liquid crystal prepared in Step 6. (The final volume should be ~1 ml.)

▲ **CRITICAL STEP** The photoinitiator should be added at this later stage to reduce its exposure to heat so as to minimize thermal degradation.

9| Evaporate the DCM using a low nitrogen stream at 60 °C for 1 h.

10| Stop the nitrogen stream and heat the mixture to 80 °C for 30 min. At this point, the mixture should be transparent to the eye, indicating that it is in the isotropic state). The liquid should then be stirred with a magnetic rod for homogeneity. After mixing, the temperature should be decreased to 48 °C gradually by setting the hot plate at such a temperature.
▲ **CRITICAL STEP** Cooling down the temperature too quickly can cause inhomogeneity in the liquid crystal mixture.

11| Label one side of the cell by attaching a small adhesive paper to the edge. This is used to label which side of the cell promotes alignment along the long axis, as this side is used as the reference to measure ϕ.

12| Wrap the cell and a metallic tip with aluminum foil, and warm them up to 60 °C by placing them in the oven for ~1 h.

13| Unwrap the prewarmed cell and place it on a hot plate preheated to 48 °C. Place a drop of liquid crystal mixture on one of the two side openings of the cell with the aid of the prewarmed metallic tip. The cell will be filled by capillary action, but the hot tip will help to fill the cell efficiently. Proceed until the cell is filled completely (**Fig. 7**). The time required to fill the cell with the mixture will depend on the nominal gap of the cell and the viscosity of the mixture, as well as the filling temperature. In the case of the liquid crystal mixture described here, which contains azo switch-1, and a 12 mm × 19 mm × 50 μm cell, the filling time is ~15 min.
▲ **CRITICAL STEP** The use of a cold metallic tip causes partial crystallization of the liquid crystal on the tip while filling the cell. The metallic tip should be prewarmed before use.
■ **PAUSE POINT** The rest of the liquid crystal mixture can be stored in the oven at 48–60 °C for about a week without any noticeable changes in properties.

14| Protect the cell from light by using aluminum foil, and leave it at 48 °C for 1 h. The liquid crystal will organize into the desired twist configuration spontaneously.

15| Fix the cell to the top of a hot plate using Scotch tape. Note whether the marked face of the cell is on the top (light-exposed face) or at the bottom (non-exposed face). The gradient formed during photopolymerization will influence the photoactuation modes of the ribbons.

16| The entire setup should be covered with a box or with aluminum foil.

17| Perform photopolymerization by irradiating the top of the cell with visible light. Ensure that the light beam covers the entire surface of the cell. Illuminate it for 90 min (**Fig. 8**).
! **CAUTION** Wear suitable eye protection while performing the irradiation with light.
▲ **CRITICAL STEP** It is critical to place a UV cutoff filter ($\lambda \geq 420$ nm) between the light source (Edmund MI-150 high-intensity illuminator) and the cell, as this minimizes *trans*-to-*cis* isomerization of Azo-1 during polymerization.
▲ **CRITICAL STEP** If the light beam does not cover the entire surface of the film, an inhomogeneous film will be formed.
? **TROUBLESHOOTING**

18| After photopolymerization, wrap the twist cell with aluminum foil and place it in an oven preheated to 60 °C overnight for postpolymerization curing.

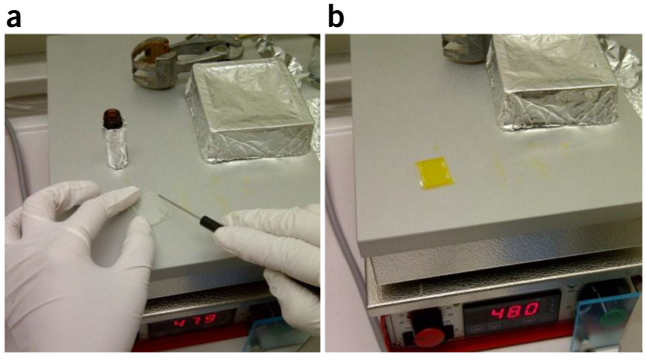

Figure 7 | Filling of the cell with the liquid crystal pre-polymer mixture. (**a**) The liquid crystal is inserted by capillary action into the cell, by using a metal tip. (**b**) The step is repeated until the cell is filled completely.

Figure 8 | Photopolymerization. The cell is irradiated ($\lambda \geq 420$ nm) at 48 °C and postcured overnight at 60 °C in the oven.

Preparation of ribbons ● **TIMING 30–45 min**

19| Fill a small Dewar flask with liquid nitrogen.
! **CAUTION** Wear suitable gloves and eye protection when you are using liquid nitrogen. Use only approved unsealed containers.

20| Soak the four corners of the cell, where the cell is glued, in liquid nitrogen. Freezing disrupts the glue and facilitates opening the cell.

21| Dry the soaked cells with tissue paper, and gently open the cell using a scalpel (**Fig. 9**).
▲ **CRITICAL STEP** The opening of the cell with a scalpel can be potentially dangerous; use caution to avoid cutting yourself or damaging the film.
▲ **CRITICAL STEP** If you have difficulty opening the cell, re-freeze the side that you wish to open in liquid nitrogen, and try again.

Figure 9 | Opening of the cell. (**a**) The cell is opened with a surgical knife, and (**b**) the liquid crystal polymer film is removed by hand from one of the cell walls.

22| After immersion in liquid nitrogen, the adhesive tape used to reference the alignment directions and to mark which side of the film was exposed to visible light (the so-called 'top-side') often detaches. Reattach the markers now.

23| Repeat Steps 19 and 20 on the other side of the cell to complete the procedure and to achieve full opening of the cell (**Fig. 9**, right). Once the cell is fully open, the film will be sitting on one of the glass slides.

24| Use a cutting board displaying different angles, and fix the glass slide supporting the film onto the cutting board with Scotch-tape. The cutting angle ϕ is defined here as the angle between the orientation of the molecules at mid-plane and the cutting direction, when the top of the film (its side that was exposed to irradiation with light) is facing up (**Fig. 3**).
▲ **CRITICAL STEP** If the liquid crystal polymer film sticks to the upper glass slide instead of sticking to the bottom glass slide, then instead of using the normal cutting angle ϕ the 'supplementary angle' $\phi_s = \pi - \phi$ should be used to predict the geometry and photoresponse of the spring.

25| Place a metallic mask along the desired cutting direction, and cut the ribbon using a razor blade (**Fig. 3**). Typically, the preparation of a ribbon involves four cuts, two for the length and two for the width of the ribbon. It is usually possible to cut multiple ribbons out of a single film.

26| Use thin tweezers to carefully remove the newly cut ribbon from the rest of the liquid crystal polymer film.

Photoactuation of ribbons ● **TIMING 30–45 min**

27| Prepare a box that is not transparent to UV light. Place the camera and the UV lamp inside the box. Use tweezers to hold the photoresponsive ribbon.
! **CAUTION** UV light is harmful to the eyes and skin; make sure that the box is sealed before UV irradiation starts.

28| Focus the camera on the ribbon.

29| Make sure that the light beam is placed so that the entire ribbon can be illuminated.
▲ **CRITICAL STEP** Use the same distance between the ribbon and the lamp for each experiment.

30| Set the parameters of the UV irradiation, such as power of the lamp and irradiation time (here we used 10% of the lamp's power and a 2-min irradiation time).

31| Record a video for the photoactuation of the ribbon.

? TROUBLESHOOTING
Occasionally, the liquid crystal polymer films can display some low-quality areas, where crystallization occurs over time (Step 30). Local crystallization can occur in the presence of dust particles or other impurities. Start the procedure again after double-checking that all consumables and chemicals are clean.

The film is occasionally too fragile, which makes it difficult to remove the ribbon from the cell wall. This can originate in the polymerization of the film being incomplete. The procedure can then be adapted by photopolymerization with a stronger lamp or by irradiating for a few minutes longer (Step 17).

● TIMING

Steps 1–18, preparation of liquid crystal polymer thin films: 1 d
Steps 19–26, preparation of ribbons: 30–45 min
Steps 27–31, photoactuation of ribbons: 30–45 min

ANTICIPATED RESULTS

The reported procedure yields distinct morphology and photoactuation of geometrical ribbons, as shown in **Figure 10**. **Supplementary Videos 1–4** show different actuation modes: winding, unwinding, helix inversion and relaxation of the spring, as discussed in the INTRODUCTION.

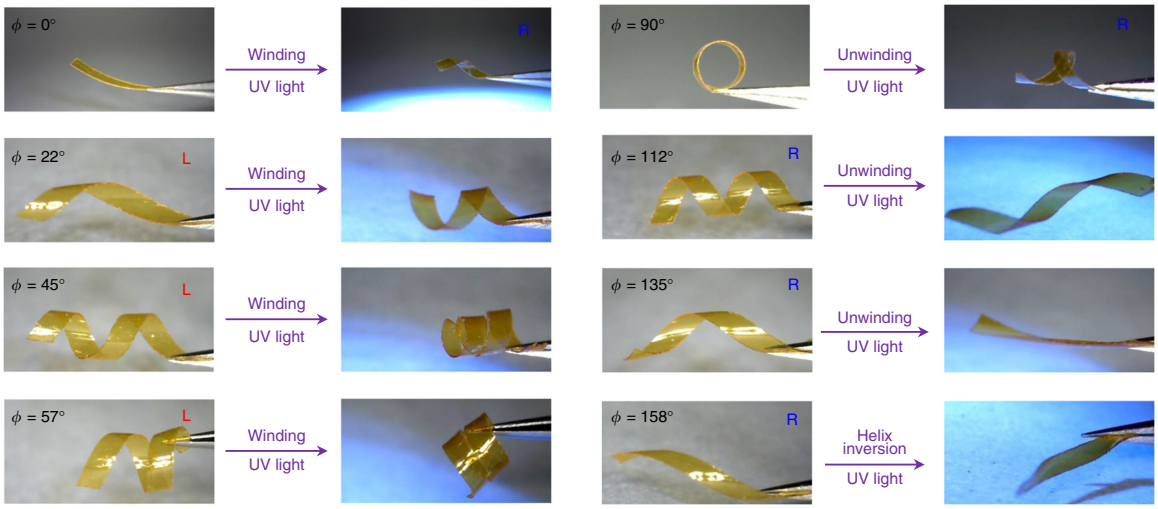

Figure 10 | The procedure allows production of a variety of photoresponsive polymer springs. Their photoresponse is encoded into their structure.

Note: Any Supplementary Information and Source Data files are available in the online version of the paper.

ACKNOWLEDGMENTS This work was supported financially by the European Research Council (Starting Grant 307784 to N.K.), the Netherlands Organization for Scientific Research (Vidi Grant to N.K.), the EPSRC (Standard Grant EP/M002144/1 to S.P.F.) and the Royal Society through an International Exchange Grant to S.P.F. and N.K. The authors gratefully acknowledge R. Carloni, A. Cremonese (Robotics and Mechatronics, University of Twente), T. Kudernac and A. Leoncini (Molecular Nanofabrication, University of Twente) for discussions on the mechanical properties of the springs.

AUTHOR CONTRIBUTIONS N.K. and S.P.F. initiated the project and designed the research. S.I., E.V., F.L. and S.-J.A. conducted the experiments and analyzed the data. F.L. conducted the tensile strength measurements. N.K., S.P.F., E.V. and F.L. wrote the manuscript and all authors contributed to discussing the results and the manuscript at all stages.

COMPETING FINANCIAL INTERESTS The authors declare no competing financial interests.

1. Finkelmann, H., Nishikawa, E., Pereira, G.G. & Warner, M.A. New opto-mechanical effect in solids. *Phys. Rev. Lett.* **87**, 015501 (2001).
2. Yu, Y., Nakano, M. & Ikeda, T. Directed bending of a polymer film by light. *Nature* **425**, 145 (2003).
3. White, T. & Broer, D.J. Programmable and adaptive mechanics with liquid crystal polymer networks and elastomers. *Nature Mater.* **14**, 1087–1098 (2015).
4. Wang, J.-S. *et al.* Hierarchical chirality transfer in the growth of the *Towel Gourd* tendrils. *Sci. Rep.* **3**, 3102 (2013).
5. Forterre, Y. & Dumais, J. Generating helices in nature. *Science* **333**, 1715–1716 (2011).
6. Isnard, S. & Silk, W.K. Moving with climbing plants from Charles Darwin's time into the 21st century. *Am. J. Bot.* **96**, 1205–1221 (2009).
7. Evangelista, D., Hotton, S. & Dumais, J. The mechanics of explosive dispersal and self-burial in the seeds of filaree erodium cicutarium. *J. Exp. Biol.* **214**, 521–529 (2011).
8. Erb, R.M., Sander, J.S., Grisch, R. & Studart, A.R. Self-shaping composites with programmable bioinspired microstructures. *Nat. Commun.* **4**, 1712 (2013).
9. Zhang, L. & Naumov, P. Light- and humidity-induced motion of an acidochromic film. *Angew. Chem. Int. Ed.* **54**, 8642–8647 (2015).
10. Zhang, L., Chizhik, S., Wen, Y. & Naumov, P. Directed motility of hygroresponsive biomimetic actuators. *Adv. Funct. Mater.* **26**, 1040–1053 (2016).
11. Wu, Z.L. *et al.* Three-dimensional shape transformations of hydrogel sheets induced by small-scale modulation of internal stresses. *Nat. Commun.* **4**, 1586 (2013).
12. de Haan, L.T *et al.* Humidity-responsive liquid crystalline polymer actuators with an asymmetry in the molecular trigger that bend, fold, and curl. *J. Am. Chem. Soc.* **136**, 10585–10588 (2014).
13. Iamsaard, S. *et al.* Conversion of light into macroscopic helical motion. *Nature Chem.* **6**, 229–235 (2014).
14. Harris, K.D. *et al.* Large amplitude light-induced motion in high elastic modulus polymer actuators. *J. Mater. Chem.* **15**, 5043–5048 (2005).

15. Yu, Y., Nakano, M., Shishido, A., Shiono, T. & Ikeda, T. Effect of cross-linking density on photoinduced bending behavior of oriented liquid-crystalline network films containing azobenzene. *Chem. Mater.* **16**, 1637–1643 (2004).
16. Dumais, J. & Forterre, Y. Vegetable dynamicks: the role of water in plant movements. *Annu. Rev. Fluid Mech.* **44**, 453–478 (2012).
17. Witztum, A. & Schulgasser, K. The mechanics of seed expulsion in *Acanthaceae*. *J. Theor. Biol.* **176**, 531–542 (1995).
18. Dawson, C., Vincent, J.F.V. & Roca, A.M. How pine cones open. *Nature* **390**, 668 (1997).
19. Elbaum, R., Zaltzman, L., Burgert, I. & Fratzl, P. The role of wheat awns in the seed dispersal unit. *Science* **316**, 884–886 (2007).
20. Studart, A.R. & Erb, R.M. Bioinspired materials that self-shape through programmed microstructures. *Soft Matter* **10**, 1284–1294 (2014).
21. Sawa, Y. *et al.* Shape selection of twist-nematic-elastomer ribbons. *Proc. Natl. Acad. Sci. USA* **108**, 6364–6368 (2011).
22. Sawa, Y. *et al.* Shape and chirality transitions in off-axis twist nematic elastomer ribbons. *Phys. Rev. E* **88**, 022502 (2013).
23. Teresi, L. & Varano, V. Modeling helicoid to spiral-ribbon transitions of twist-nematic elastomers. *Soft Matter* **9**, 3081–3088 (2013).
24. Wie, J.J. *et al.* Torsional mechanical responses in azobenzene functionalized liquid crystalline polymer networks. *Soft Matter* **9**, 9303–9310 (2013).
25. van Oosten, C.L. *et al.* Bending dynamics and directionality reversal in liquid crystal network photoactuators. *Macromolecules* **41**, 8592–8596 (2008).
26. Liu, D. & Broer, D.J. Liquid crystal polymer networks: preparation, properties, and applications of films with patterned molecular alignment. *Langmuir* **30**, 13499–13509 (2014).
27. Liu, D. & Broer, D.J. New insights into photoactivated volume generation boost surface morphing in liquid crystal coatings. *Nat. Commun.* **6**, 8334 (2015).
28. Sanchez-Ferrer, A., Merekalov, A. & Finkelmann, H. Opto-mechanical effect in photoactive nematic side-chain liquid-crystalline elastomers. *Macromol. Rapid Commun.* **32**, 671–678 (2011).
29. Zeng, H. *et al.* High-resolution 3D direct laser writing for liquid-crystalline elastomer microstructures. *Adv. Mater.* **26**, 2319–2322 (2014).
30. Min Lee, K., Lynch, B.M., Luchette, P. & White, T.J. Photomechanical effects in liquid crystal polymer networks prepared with *m*-fluoroazobenzene. *J. Polym. Sci. A* **52**, 876–882 (2014).
31. Shadmehr, R. & Arbib, A.M. A mathematical analysis of the force-stiffness characteristics of muscles in control of a single joint system. *Biol. Cybern.* **66**, 463–477 (1992).
32. Mossety-Leszczak, B., Wlodarska, M., Galina, H. & Bak, G.W. Comparing liquid crystalline properties of two epoxy compounds based on the same azoxy group. *Mol. Cryst. Liq. Cryst.* **490**, 52–66 (2008).
33. Li, C. *et al.* Synthesis of a photoresponsive liquid-crystalline polymer containing azobenzene. *Macromol. Rapid Commun.* **30**, 1928–1935 (2009).